

## 31. ALTERATION OF BASALT: DEEP SEA DRILLING PROJECT LEGS 64 AND 65<sup>1</sup>

M. Ann Morrison<sup>2</sup> and R. N. Thompson, Imperial College of Science and Technology,  
London SW7 2BP, United Kingdom

### INTRODUCTION

Evidence for submarine hydrothermal activity along oceanic spreading centers has been accumulated from a large and diverse body of geochemical and geophysical data (e.g., Boström and Peterson, 1966; Wolery and Sleep, 1976; Humphris and G. Thompson, 1978), and the alteration of oceanic rocks by seawater has been the subject of intense study for the last few years. Previous studies of Deep Sea Drilling Project (DSDP) samples have found little evidence of high-temperature hydrothermal activity in the upper part of the oceanic crust. Instead, most of the alteration described appears to be the result of low-temperature interchange between basalt and seawater under ambient conditions on the seafloor. This type of alteration is most pronounced along fractures and open channelways and involves the growth of smectite, carbonate, and occasionally pyrite and phillipsite. Olivine crystals and interstitial glassy material within the basalts are frequently replaced by smectites and more rarely, carbonate, but the plagioclase feldspars and clinopyroxenes are normally unaffected. The resulting chemical changes usually involve notable increases in H<sub>2</sub>O, Fe<sub>2</sub>O<sub>3</sub>, K<sub>2</sub>O, Rb, Cs, and U and smaller increases in total iron and Sr. TiO<sub>2</sub>, Al<sub>2</sub>O<sub>3</sub>, P<sub>2</sub>O<sub>5</sub>, Nb, Zr, and Y are usually considered to be little affected by alteration (e.g., Bass, 1976; Robinson et al., 1977). Several workers (e.g., Pritchard et al., 1979) have noticed an increase in the degree of alteration with age.

In contrast, DSDP Legs 64 and 65 found evidence for local hydrothermal activity at a high level in the ocean crust at several localities in the Guaymas Basin and at the mouth of the Gulf of California. Although most of the basalts recovered contained the assemblage smectite, carbonate, and pyrite and were considered to show typical low-temperature alteration, evidence for intense hydrothermal activity was reported from sediments adjacent to sill-like intrusions in the Guaymas Basin (Einsle et al., 1980) and local alteration of basalt to chlorite and actinolite was observed at Site 482 at the mouth of the Gulf. Although these samples represented the first reported occurrence of hydrothermally altered basalts in DSDP drill holes in "normal" ocean crust, they were not thought to be representative of the alteration processes operating along this section of the East Pacific

Rise. Subsequent work suggests that many of the other basalts sampled by Legs 64 and 65 were also affected by hydrothermal alteration. The main purpose of this chapter is to describe the alteration of these basalts in terms of their mineralogy and chemistry and to compare them with samples recovered from other DSDP sites.

### SAMPLING AND ANALYTICAL TECHNIQUES

To accomplish these objectives, 69 bulk-rock samples were collected for microprobe and fluorescence spectrometer analysis from Sites 482, 483, and 485 at the mouth of the Gulf during Leg 65. Wherever possible, multiple samples were taken from individual cooling units that showed variable degrees of alteration. No attempt was made to sample all of the chemical and lithological types recognized on ship, but the set is fairly representative of the compositional range encountered. These were supplemented by 13 samples of fresh glass in order to determine the initial compositions of the rocks. In addition, a set of 21 basalt samples and 7 glass samples were made available to us from Holes 474A, 477A, and 478, enabling us to investigate the nature of the alteration processes operating in the Guaymas Basin.

The electron microprobe analyses were made at Imperial College, using a Cambridge Instruments Microscan V probe fitted with a Link EDS detector. The probe was operated at an accelerating voltage of 15 kV, a specimen current of 0.01  $\mu$ A, and a counting time of 100 s. The beam was focused to a minimum spot except when analyzing hydrous secondary minerals and carbonates, at which time a defocused beam was used. Microprobe analysis of secondary minerals poses special problems because of their high volatile content, small grain size, and inhomogeneity, either in the minerals or in the polishing. For most of the analyses reported here, the beam was defocused to 40  $\mu$ m to reduce decomposition; nevertheless, some decomposition was always observed. The only instance in which loss of alkalis was detected was in the zeolites from Hole 478 (Table 1) where a slight loss of Na with time was observed. A defocused beam could not be used for the sulfates in Hole 482C because the crystals were too small. Nevertheless, the analyses reported here showed a high degree of repeatability and, except for the reservations noted, are believed to be reasonably accurate.

Table 1. Defocused microprobe analyses of smectites and zeolites from Hole 478.

Oxide	1	2	3	4	5	6	7	8
SiO <sub>2</sub>	34.96	33.63	33.20	43.58	48.26	41.01	44.17	40.70
TiO <sub>2</sub>	0.05	0.05	—	—	0.02	—	0.04	—
Al <sub>2</sub> O <sub>3</sub>	12.65	9.63	13.20	25.85	8.37	27.18	27.60	27.40
FeO*	20.35	18.30	22.12	0.13	0.10	0.15	0.14	0.45
MnO	0.19	0.38	0.20	—	0.01	—	—	0.10
MgO	12.59	12.41	8.74	0.08	0.04	0.06	0.21	0.65
CaO	5.41	2.62	6.09	10.48	25.72	11.37	7.01	11.52
Na <sub>2</sub> O	0.60	1.06	0.84	4.27	1.78	2.67	5.97	3.90
K <sub>2</sub> O	0.11	0.13	0.29	0.05	0.08	—	0.06	0.18
Total	86.81	78.21	84.68	84.44	84.38	82.44	85.20	84.90

Note: All analyses from Sample 478-45-3, 67-71 cm; 1-3, green smectites in groundmass; 4, zeolite replacing plagioclase (1) in Table 2; 5-7, zeolites replacing plagioclase (2) in Table 2; 8, groundmass zeolites. Values shown in wt. %.

<sup>1</sup> Lewis, B. T. R., Robinson, P., et al., *Init. Repts. DSDP, 65*: Washington (U.S. Govt. Printing Office).

<sup>2</sup> Department of Geological Sciences, University of Birmingham, P.O. Box 363, Birmingham B15 2TT, United Kingdom.

Major and trace element analyses were obtained using the Phillips 1212 X-ray fluorescence spectrometer at Imperial College. The Li and Sc data were obtained at Kings College, London, using an inductively coupled plasma spectrometer. Details of the analytical techniques have been published elsewhere and will not be reported in detail here. (Flower et al., 1979; Walsh, 1980). FeO determinations were carried out using the method of Whipple (1974).

Loss of ignition was determined for each sample by first drying the powder at 110°C for 24 hr. and then igniting it in a furnace at 1000°C until constant weights were obtained. The weight losses were corrected for the effects of oxidation of FeO during ignition.

## SECONDARY MINERALS

### The Guaymas Basin

The Guaymas Basin is an active spreading center formed during the last 3.5 m.y. and characterized by high sedimentation rates—in excess of 1200 m/m.y. Samples were obtained from a dolerite sill near the top of Hole 477A in the southern rift and from a massive dolerite sill at the base of Hole 478, which was drilled 12 km from Site 477 on the basin floor northwest of the south rift. Einsele et al. (1980) have presented convincing evidence that the intrusion of sills into the highly porous sediments of the Guaymas Basin was accompanied by thermal alteration of the sediments, marked changes in interstitial water chemistry, and large-scale expulsion of heated pore fluids. This process is thought to have created space for the intruding magmas and to have initiated hydrothermal systems which gave rise to the deposits of talc, pyrrhotite, and sulfides observed near fault scarps on the basin floor. Various changes have been recorded in the sediments adjacent to the sills sampled in this study, including the remobilization of silica, the formation of dolomite, and the recrystallization of clay minerals. Temperatures in the sediments are thought to have reached values of approximately 150°C.

Despite the locally intense thermal alteration suffered by the sediments, the basalts contain only minor amounts of secondary minerals. The Hole 477A samples contain small quantities of smectite and carbonate as fillings in radial fractures and as secondary minerals replacing olivine and groundmass material. *Unfilled* vesicles were observed just below the chilled margin. The samples from Hole 478 show similar amounts of smectite and, in addition, contain zeolites replacing both plagioclase and groundmass material. Microprobe analyses of these minerals are listed in Tables 1 and 2 and the compositional variations are shown in Figures 1 and 2.

Both the smectites and the zeolites in the Hole 478 samples show distinct differences in composition from the analyses reported for other DSDP sites. The zeolite species normally encountered in ocean floor basalts is the K-rich variety, phillipsite. In the K<sub>2</sub>O–Na<sub>2</sub>O–CaO plot shown in Figure 1, they plot close to the base of the triangle, overlapping the plagioclase compositions from the same samples. When allowance is made for the possibility of Na loss during analysis as previously discussed, it seems likely that the spread of the zeolites towards the CaO apex is probably only an artifact. The smectites show a similar impoverishment in potassium relative to smectites from other DSDP sites with a similar FeO\*/MgO ratio. With the exception of the smectites

Table 2. Composition of groundmass plagioclases, Hole 478.

Oxide	Cations per		Cations per	
	1	Eight Oxygens	2	Eight Oxygens
SiO <sub>2</sub>	58.01	2.60	58.87	2.63
TiO <sub>2</sub>	0.14	—	0.03	—
Al <sub>2</sub> O <sub>3</sub>	26.00	1.37	25.24	1.33
FeO*	0.50	0.02	0.47	0.02
MnO	—	—	—	—
MgO	0.09	0.01	0.19	0.01
CaO	8.30	0.40	7.72	0.37
Na <sub>2</sub> O	6.81	0.59	7.23	0.63
K <sub>2</sub> O	0.11	0.01	0.23	0.01
Total	99.94	5.00	100.04	5.00

Note: Values shown in columns 1 and 2 are in wt. %.

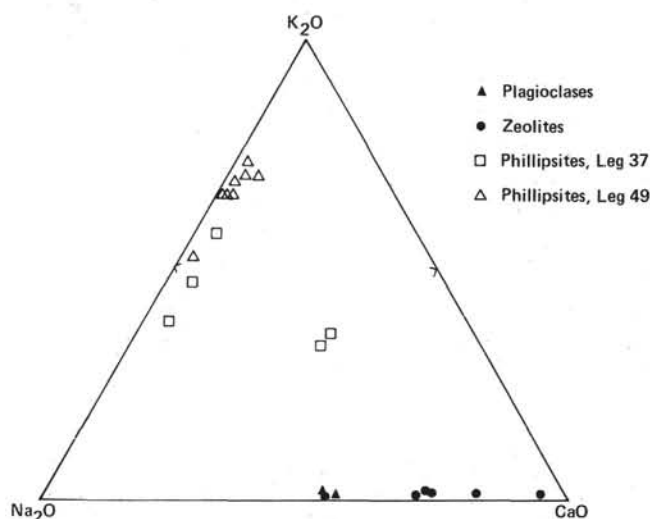


Figure 1. Distribution of plagioclases and zeolites from Hole 478 on a K<sub>2</sub>O–Na<sub>2</sub>O–CaO diagram. (Also shown are phillipsites from Legs 37 and 49. Data sources: Scarfe and Smith, 1977; Robinson et al., 1977; Pritchard et al., 1979.)

from Site 483, which will be discussed later, this seems to be a characteristic of the clay minerals recovered during Legs 64 and 65.

### Site 474

Site 474 was located approximately 5 km from the continent/ocean-crust transition near the southeast tip of Baja California. The basalts sampled at this site represent the oldest material recovered from the ocean floor along the transect across the mouth of the Gulf of California. The sedimentation rates, although high, are significantly lower here than in the Guaymas Basin, and some extrusion of basalt occurred directly on the seafloor. Consequently, little of the intense sediment alteration noted in the Basin has been reported for this site. The average sedimentation rate at Site 474 was 160 m/m.y., but the rate increased during the Quaternary to 240 m/m.y. The drilling in Hole 474A penetrated a thick sedimentary sequence, followed by a few massive units and then interbedded pillows and massive basalts. A similar basement stratigraphy was encountered at the other sites drilled along the transect during Leg 65,

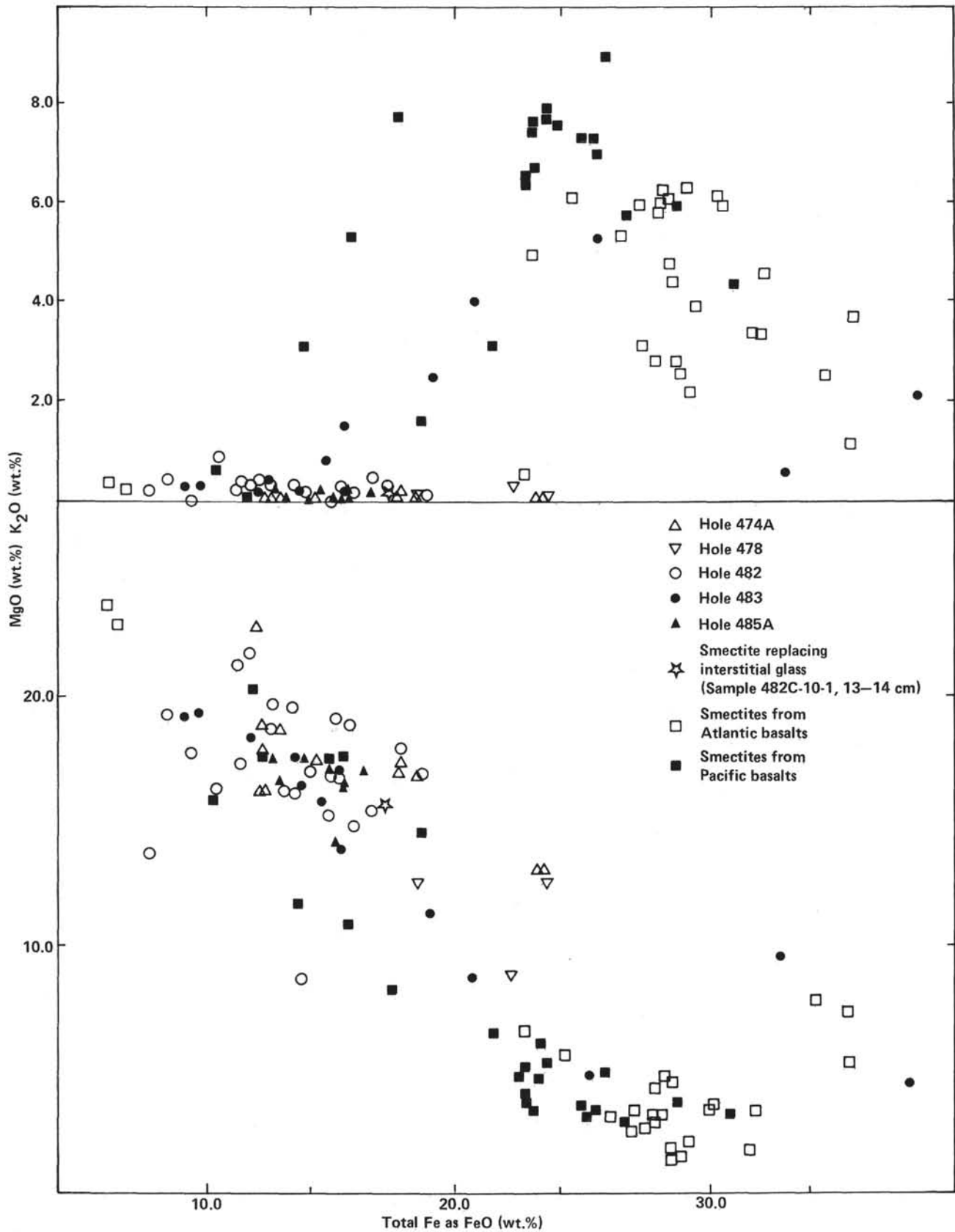


Figure 2. MgO and K<sub>2</sub>O versus total iron as FeO\* for smectites in basalts from Legs 64 and 65. (Also shown are typical smectite compositions from basalts affected by low-temperature alteration from both the Atlantic and Pacific oceans. Values shown in wt.%. Data sources: Pritchard et al., 1979; Humphris et al., 1980; Robinson et al., 1977.)

showing this structure to be typical of this section of the East Pacific Rise.

Other than the possible occurrence of minor chlorite in veins (reported by the shipboard party but not confirmed by subsequent study), the basalts recovered from Hole 474A appeared to show typical low-temperature secondary mineral assemblages. Fresh glass selvages showing little or no palagonitization were recovered from several intervals, and many of the samples contained fresh olivine. Altered intervals of the drill core show replacement of olivine and groundmass glass by green brown smectites, and the growth of smectites and carbonate in veins and vesicles. Detailed examination of thin sections, however, revealed that in several instances, the groundmass clinopyroxenes had also been partially replaced by smectite and that the plagioclases contain veins and patches of smectites growing along cleavage cracks and around the margins. The most intense alteration was seen in Core 50 from which two samples were collected. The lower sample, 474A-50-3, 103–106 cm, consists of a fine-grained, phyrlic, variolitic basalt containing approximately 10 modal percent plagioclase phenocrysts and possible olivine microphenocrysts in a matrix of quench-textured clinopyroxene sheaves, altered olivines, opaques, and smectite. The upper sample, 474A-50-2, 133–145 cm, is petrographically very similar, except for the fact that the clinopyroxene has been completely replaced by smectite.

Representative analyses of the smectites and carbonate are given in Table 3 and shown in Figure 2. Like the smectites from Hole 478 in the Guaymas Basin, they occupy a rather restricted range of relatively Mg-rich compositions compared to samples from other DSDP sites and show no evidence of increasing K<sub>2</sub>O content with increasing total iron.

#### Site 482

Site 482 was located approximately 12 km east of the East Pacific Rise in a sediment-filled valley south of the Tamayo Fracture Zone. The age of the crust is no greater than 0.5 m.y., and the sediment accumulation rates range between 340 and 550 m/m.y. A temperature of approximately 90°C was estimated for the basalt/sediment contact from shipboard measurements. Drill-

ing at the site, however, opened a conduit through the sediments through which hot water flowed upward to form a small hot-spring on the ocean floor. The presence of this manmade spring was detected by temperature sensors in the Hawaiian downhole seismometer package which measured an equilibrium temperature of ~150°C near the bottom of Hole 482C. This clearly demonstrates that relatively high-temperature fluids are still circulating in the crust at Site 482 (Duenebier and Blackinton, 1980).

Basalts were successfully recovered from four of the holes drilled at Site 482. Several units could be correlated between holes on the basis of their lithologic, chemical, and magnetic properties. An upper aphyric unit which was 22 meters thick in Hole 482B, 24 meters thick in Hole 482C, and 29 meters thick in Hole 482D was underlain by a sequence of sparsely plagioclase-aphyric basalts which were 18, 26, and 39 meters thick in Holes 482D, C, and B respectively. Farther down in the basement, thin cooling units predominate in all three holes. In addition, similar distributions of secondary minerals were seen in each of the holes. Pyrite, for example, is abundant just below the sediment/basement interface in all three holes. It is disseminated in the basalt groundmass and also occurs as vein and vesicle fillings. Veins of smectite, pyrite, and carbonate are particularly abundant. The abundance of the sulfides decreases rapidly down all three holes, only to reappear abruptly just below the next sediment/basalt interface.

In Section 482C-10-2, a large vein occurs in the upper 24 cm which splits a preexisting segregation vein. The vein has a prominent alteration halo and occurs in the same massive basalt unit as a patch of high-temperature secondary minerals. The sequence of minerals infilling this vein consists of finely disseminated sulfides, smectite and opal, pyrite, calcite, and barite. With the exception of the calcite (which is ubiquitous on the ocean floor), this is precisely the same mineral assemblage as that currently being discharged as particulate material from the group of active hydrothermal vents on the East Pacific Rise at 21°N known as the "white smokers." Temperatures of approximately 300°C were measured in these vents during the RISE expedition of 1979 (Haymon and Kastner, 1981). Paleotemperatures of this mag-

Table 3. Defocused microprobe analyses of smectites and carbonate, Hole 474A.

Oxide	1	2	3	4	5	6	7	8	9	10	11	12
SiO <sub>2</sub>	45.96	49.21	46.87	50.13	47.63	48.11	50.11	50.30	53.39	52.33	51.44	0.10
TiO <sub>2</sub>	0.14	0.12	—	0.12	—	0.32	0.11	0.04	0.02	—	0.10	—
Al <sub>2</sub> O <sub>3</sub>	4.39	4.77	4.39	3.95	5.23	3.29	0.15	—	0.20	0.11	2.90	—
FeO*	12.14	12.75	12.08	12.07	14.19	22.95	23.28	23.20	17.59	18.22	17.48	0.73
MnO	0.09	0.10	0.07	0.07	—	0.18	0.16	0.14	0.22	0.17	0.15	3.47
MgO	17.31	18.86	18.06	18.91	17.52	11.87	13.08	13.03	17.54	16.82	17.00	0.60
CaO	0.61	0.10	0.13	0.20	0.18	1.21	0.72	0.63	0.29	0.40	0.81	50.49
Na <sub>2</sub> O	1.11	1.94	1.74	1.57	2.02	0.95	0.37	0.34	0.58	0.50	0.64	0.16
K <sub>2</sub> O	0.10	0.09	0.11	0.07	0.08	0.09	0.12	0.10	0.17	0.10	0.12	—
Total	81.85	87.94	83.45	87.09	86.85	88.97	88.10	87.78	89.24	88.65	90.64	55.55

Note: 1, groundmass smectite, Sample 474A-50-2, 133–135 cm; 2, green brown smectite around vesicle rim, Sample 474A-50-2, 133–135 cm; 3, smectite in center of same vesicle; 4, brown smectite around vesicle rim, Sample 474A-50-2, 133–135 cm; 5, smectite in center of same vesicle; 6, green smectite replacing groundmass plagioclase, Sample 474A-50-3, 103–106 cm; 7–10, smectites replacing olivines, Sample 474A-50-3, 103–106 cm; 11, groundmass smectite, Sample 474A-50-3, 103–106 cm; 12, carbonate in center of same vesicle as 2 and 3. Values shown in wt. %.

Table 4. Defocused microprobe analyses of smectites, Site 482.

Oxide	1	2	3	4	5	6	7	8	9	10	11	12	13	14	15	16	17	18	19	20	21	22	23	24	25	26
SiO <sub>2</sub>	48.57	45.79	50.03	50.68	44.53	45.15	44.12	44.21	46.12	43.16	42.39	43.09	43.67	42.17	42.87	42.79	55.48	55.88	55.45	51.31	41.36	38.24	36.62	43.68	49.98	38.97
TiO <sub>2</sub>	0.06	0.13	0.20	0.08	1.29	0.12	0.14	3.38	0.66	0.08	0.08	—	0.27	0.02	0.34	—	0.09	—	—	0.06	—	0.15	0.11	1.70	0.04	0.01
Al <sub>2</sub> O <sub>3</sub>	4.96	2.73	2.45	2.89	4.66	3.59	9.96	11.35	9.65	4.71	4.96	4.51	5.49	5.86	5.89	0.04	—	—	1.32	8.39	10.88	10.08	4.19	3.46	10.53	
FeO*	10.26	11.09	11.78	12.36	9.07	8.19	17.02	13.64	7.47	15.73	14.67	13.39	16.37	15.12	14.79	12.89	11.50	10.99	11.67	12.53	18.65	17.59	15.05	14.03	13.35	15.63
MnO	—	0.38	0.13	—	0.10	0.04	0.15	0.19	0.19	0.09	0.02	0.20	0.09	0.12	0.19	0.02	0.12	0.08	0.17	0.34	0.17	0.37	0.03	0.15	0.18	0.21
MgO	17.36	18.28	18.98	19.76	18.75	19.26	15.70	8.62	13.71	14.86	15.21	16.05	15.17	16.89	15.87	16.14	21.72	21.43	21.02	19.74	17.00	18.02	19.21	17.07	19.61	18.98
CaO	1.11	3.04	1.02	1.19	1.63	0.70	1.87	4.25	3.68	0.78	0.86	0.77	1.26	0.66	1.12	1.60	0.28	0.37	0.09	2.20	1.05	0.88	0.51	1.56	0.84	0.97
Na <sub>2</sub> O	0.44	0.28	0.28	0.12	0.04	0.56	0.57	3.69	1.93	1.38	1.42	1.39	1.10	1.39	1.47	0.60	0.46	0.32	0.17	0.23	0.31	0.29	0.16	0.59	0.34	0.13
K <sub>2</sub> O	0.82	0.39	0.43	0.27	0.04	0.19	0.14	0.15	0.13	0.14	0.01	0.18	0.24	0.29	0.12	0.05	0.27	0.23	0.21	0.23	0.15	0.11	0.11	0.26	0.14	0.11
Total	83.58	82.11	85.30	87.35	80.11	77.80	89.67	89.48	83.54	80.93	79.62	79.63	82.68	82.15	82.63	79.89	89.96	89.30	88.87	87.96	87.08	86.53	81.88	83.23	87.94	85.54

Note: 1, groundmass smectite, Sample 482B-10-7, 81–86 cm; 2, brown smectite replacing olivine, Sample 482B-10-7, 81–86 cm; 3, 4, brown smectites in groundmass, Sample 482B-10-7, 81–86 cm; 5, smectite in groundmass, Sample 482C-9-1, 76–77 cm; 6, smectite in groundmass, Sample 482C-10-1, 13–14 cm; 7, smectite replacing interstitial glass, Sample 482C-10-1, 13–14 cm; 8, vesicle filling, Sample 482C-10-1, 16–18 cm; 9, smectite replacing clinopyroxene, Sample 482C-10-1, 16–18 cm; 10–14, green smectites in groundmass, Sample 482C-11-2, 71–75 cm; 15, 16, brown smectites in groundmass, Sample 482C-11-2, 71–75 cm; 17–21, sequence of analyses from the center to the rim of a smectite pseudomorph after an olivine phenocryst, Sample 482C-11-4 98–102 cm; 22–26 smectites in groundmass, Sample 482C-11-4, 98–102 cm. Values shown in wt. %.

nitide would agree well with the occurrence of green-schist-facies minerals near the sediment/basalt contact in Hole 482C. Accordingly, our sampling at Site 482 concentrated on this upper unit, particularly the section drilled in Hole 482C from which 10 samples were taken. A few samples were taken from lower units in Holes 482B and D.

Representative analyses of the secondary minerals found at Site 482 are given in Tables 4 through 8. Although samples were taken from the same pieces of core as the shipboard thin sections showing hydrothermal alteration, the only secondary minerals observed were pyrite, smectite, carbonate, and opal. The opal occurs in Sample 482C-10-1, 16–18 cm, close to the large hydrothermal vein. No analyses could be obtained of it, however, since it is too finely disseminated within the groundmass to be isolated. The carbonates and smectites, both within the veins and the groundmass, are compositionally similar to those seen in Holes 474A and 478 (Tables 3, 4, and 6 and Fig. 2). The smectites from the samples which show high-temperature alteration plot in the middle of the groups seen in Figure 2 as do the smectites observed replacing groundmass pyroxenes in Sections 474A-50-3 and 50-2. These particular samples (Samples 482C-11-1, 101–105 cm and 482C-11-2, 71–75 cm), also show bulk compositional trends indicative of high-temperature alteration.

Outside the alteration halo associated with the hydrothermal vein in Core 482C-10, small patches of relict interstitial glass were found. The average composition of this glass is compared with that of the smectites replacing it in Table 5. If  $1/P_2O_5$  is taken as an index of frac-

Table 5. Comparison between unaltered interstitial glass and associated smectite, Sample 482C-10-1, 16–18 cm, both recalculated to 100%.

Oxide	Glass	Smectite	Effect of Alteration
SiO <sub>2</sub>	60.91	49.17	—
TiO <sub>2</sub>	2.69	0.16	—
Al <sub>2</sub> O <sub>3</sub>	11.92	11.10	Little change
FeO*	14.04	18.97	+
MnO	0.27	0.17	—
MgO	1.70	17.50	++
CaO	5.80	2.08	—
Na <sub>2</sub> O	0.93	0.64	(-)
K <sub>2</sub> O	0.85	0.16	—
P <sub>2</sub> O <sub>5</sub>	0.89	0.05	—

Table 6. Defocused microprobe analyses of carbonates, Site 482.

Oxide	1	2	3	4	5	6	7	8	9
FeO*	1.00	1.15	—	0.98	0.64	—	0.06	0.17	0.07
MnO	2.77	2.71	1.51	4.46	3.80	1.09	1.44	1.91	1.60
MgO	2.27	2.23	0.58	3.05	1.92	0.58	0.91	0.58	0.52
CaO	47.64	47.57	51.21	45.18	46.33	51.76	51.25	50.18	51.29
Total	53.68	53.66	53.30	53.67	52.69	52.91	53.66	52.84	53.48

Note: 1, fibrous carbonate at edge of pyrite vein, Sample 482B-10-7, 24–27 cm; 2, well-formed carbonate crystals in center of same vein; 3, carbonate in hydrothermal vein, Sample 482C-10-1, 13–14 cm; 4–8, groundmass carbonates, Sample 482C-10-1, 16–18 cm; 9, carbonate in hydrothermal vein, Sample 482C-10-1, 16–18 cm. Values shown in wt. %.

tional crystallization, then comparison of this glass with the bulk composition of the host basalt suggests that it represents the residue after approximately 70% solidification. Such glasses are rarely recovered unaltered from the ocean floor. Examination of Table 5 shows that the alteration of this interstitial glass involves an extensive loss of Si and Ca and a considerable gain in Mg. Potassium is also leached. These chemical changes are the same as those documented by Humphris and Thompson (1978) for the hydrothermal alteration of ocean floor basalts by seawater. In contrast, the low-temperature replacement of basaltic glass by palagonite typically involves an increase in K<sub>2</sub>O and a loss in Mg (Pritchard et al., 1979).

### Site 483

Site 483 is located about 52 km west of the East Pacific Rise crest and about 25 km east of the base of the continental slope off Baja California. The basement structure is similar to that found at Sites 474 and 482—a sequence of interbedded sediments, massive flows, and pillow lavas, with the abundance of igneous rocks increasing downhole and good lateral correlation between adjacent holes. The calculated sedimentation rate (62 m/m.y.) is considerably lower than at the other sites.

At first glance the alteration of the basalts appears to be similar to that documented at the other sites. Pervasive alteration has resulted in the replacement of olivine and interstitial glass by smectites (Table 9) and minor carbonate. Veins and selvages are filled by, or partly altered to, smectite and carbonate. The amount of alteration increases downhole, but no systematic change was noted in grade of alteration. In addition, the groundmass and vesicles locally contain mixed precipitates of iron hydroxides and silica, indicating very strong oxidation (Table 10). Similar minerals resembling limonite in

Table 7. Microprobe analyses of sulfides, Site 482.

Element	1	2	3	4	5	6	7	8	9	10	11	12	13	14	15	16	17	18	19	20	21	22	23	24	25
Mg	0.08	—	—	0.01	0.16	—	—	0.04	0.08	0.06	0.04	0.09	0.08	0.04	0.17	0.04	0.07	0.04	—	0.09	0.07	0.06	—	—	0.07
Si	0.16	0.14	0.03	0.10	0.06	0.10	0.09	0.12	0.10	0.02	0.10	0.09	0.18	0.04	0.43	0.18	0.11	0.13	0.02	0.13	0.08	0.08	0.09	0.13	0.14
S	51.35	51.91	51.64	51.76	52.30	53.12	52.51	50.96	52.68	51.88	52.99	52.39	52.83	51.82	51.34	52.10	52.61	51.21	52.42	52.74	51.65	51.95	52.02	52.02	52.31
Fe	47.48	45.43	47.23	47.08	47.70	47.91	47.82	46.85	48.16	47.37	48.11	47.44	46.79	47.95	47.07	47.40	46.52	46.49	45.99	47.77	47.25	47.28	47.89	47.47	47.88
Ni	—	—	—	—	—	—	—	—	0.11	—	—	—	—	—	0.05	0.02	—	0.03	—	—	—	0.06	0.27	0.08	0.06
Mn	0.08	1.39	0.07	0.25	—	0.26	—	—	0.01	0.02	0.05	0.07	0.86	—	—	0.93	0.15	1.44	0.05	—	—	—	0.02	—	—
Zn	0.47	—	—	0.44	0.47	—	—	0.10	0.18	0.08	0.17	0.28	0.12	0.17	0.08	0.10	0.35	0.32	0.17	0.38	0.14	—	0.24	0.15	0.27
Total	99.62	98.87	98.97	99.64	100.69	101.39	100.42	98.07	101.32	99.43	101.46	100.36	100.86	100.02	99.14	99.84	100.59	98.37	99.67	101.16	99.18	99.43	100.53	99.85	100.73

Note: 1, 2, sulfides in groundmass, Sample 482B-10-7, 24-27 cm; 3, 4, sulfide crystals in hydrothermal vein, Sample 482B-10-7, 24-27 cm; 5-9, sulfides in groundmass, Sample 482B-12-1, 32-36 cm; 10-19, traverse from altered basalt into hydrothermal vein, with 10-15 being sulfide crystals in groundmass and 16-19 being sulfides in vein sequence, Sample 482C-10-1, 16-18 cm; 20-25, sulfides in groundmass, Sample 482C-11-2, 71-75 cm.

Table 8. Microprobe analyses of barites, Hole 482C.

Oxide	1	2	3
MgO	—	—	—
Al <sub>2</sub> O <sub>3</sub>	—	0.15	0.08
SiO <sub>2</sub>	0.28	0.40	0.35
SO <sub>3</sub>	35.64	34.72	34.73
CaO	—	0.05	—
BaO	66.44	65.97	64.81
FeO	—	—	—
Total	102.36	101.29	99.97

Note: All analyses are of crystals from the center of a hydrothermal vein, Sample 482C-10-1, 16-18 cm.

thin section have been reported from Atlantic basalts affected by low-temperature alteration by Humphris et al. (1980), who attributed the formation of limonite to the slow percolation of cold seawater through veinlets and vesicles containing sulfides. No sulfides were observed in the oxidized samples from Site 483.

Examination of Figure 2 shows that the smectites in the Site 483 basalts follow a totally different trend from those followed by the basalts from the other sites. Instead, they resemble the smectites described from Pacific and Atlantic basalts affected by low-temperature alteration in that they exhibit a strong increase in both K<sub>2</sub>O and total iron. They also exhibit the widest range of FeO\*/MgO ratios seen in the clay minerals from Legs 64 and 65.

#### Site 485

Site 485 was located approximately 12 km east of Site 482 on crust less than 1 m.y. old. The upper part of the

basement consists of interlayered massive basalts and sediments. The massive basalts are similar to those found at Sites 482, 483, and 474 except that they are thicker and much more coarse grained. Most of the basalts again appear to exhibit low-temperature alteration characterized by the replacement of olivine and interstitial glass by smectite and minor carbonate. Nevertheless, it can be seen from Table 11 and Figure 2 that the smectites duplicate the trends shown by those from Sites 474 and 482 rather than Site 483. In addition, evidence for hydrothermal activity was noted in several sections of the core: Sample 485-17-2, 60-70 cm contains a hydrothermal breccia with fragments of basalt in a matrix of calcite. A vein of smectite containing small euhedral crystals of epidote occurs in Sample 485-24-1, 69-81 cm and minor amounts of actinolite and chlorite were reported replacing clinopyroxene, particularly in the lower part of the core.

#### BULK CHEMICAL CHANGES DURING ALTERATION

The main problem in documenting the effects of alteration on the chemistry of the basalts studied here consists in distinguishing these effects from primary differences in composition. Most of the basalts sampled were massive flows or sills which appear to have been considerably affected by *in situ* fractionation. Even with thin cooling units or pillows the problem cannot be entirely eradicated.

#### Glass-Basalt Comparisons

Figure 3 shows the major element variation exhibited by the glasses analyzed during the course of this study. Despite their extremely small range of MgO contents (less than 1 wt.%) the glasses exhibit two subparallel

Table 9. Defocused microprobe analyses of smectites, Site 483.

Oxide	1	2	3	4	5	6	7	8	9	10	11	12
SiO <sub>2</sub>	45.76	48.35	47.62	34.79	48.69	49.23	47.52	34.40	47.64	47.78	46.98	48.82
TiO <sub>2</sub>	0.22	0.06	0.01	0.39	—	0.10	0.11	0.03	—	0.08	0.14	0.05
Al <sub>2</sub> O <sub>3</sub>	3.37	3.62	4.03	3.69	4.01	4.00	4.66	2.47	4.26	4.69	3.61	3.74
FeO*	13.52	15.24	11.70	33.00	14.48	18.59	15.30	38.30	8.95	20.49	25.27	9.46
MnO	0.02	0.15	—	0.05	0.07	0.02	—	0.12	0.04	0.04	0.12	—
MgO	16.50	17.12	18.28	9.74	15.90	11.37	13.87	4.55	19.26	7.80	4.79	19.38
CaO	1.15	1.35	0.98	3.77	1.19	1.15	1.63	1.50	1.23	1.42	0.95	1.17
Na <sub>2</sub> O	0.23	0.18	0.58	0.94	0.13	0.34	0.27	0.17	0.20	0.25	—	0.33
K <sub>2</sub> O	0.20	0.20	0.13	0.63	0.83	2.50	1.53	2.14	0.24	4.06	5.36	0.27
Total	80.97	86.27	83.33	87.00	85.30	87.30	84.89	83.68	81.82	86.61	87.22	83.22

Note: 1, smectite in groundmass, Sample 483B-18-1, 27-31 cm; 2, brown vein cutting feldspar, Sample 483B-18-1, 27-31 cm; 3, 4, center and rim of olivine crystal replaced by dark brown smectite, Sample 483B-32-2, 116-123 cm; 5, 6, orange brown smectites in groundmass, Sample 483B-32-2, 116-123 cm; 7, 8, brown smectite after olivine, Sample 483B-32-2, 135-141 cm; 9, green smectite after olivine, Sample 483B-32-2, 135-141 cm; 10, smectite in groundmass, Sample 483B-32-2, 135-141 cm; Sample 11, 12, olivine replaced by green brown smectite, Sample 483B-32-2, 135-146 cm. Values shown in wt. %.

Table 10. Defocused microprobe analyses of limonite, Hole 483B.

Oxide	1	2	3
SiO <sub>2</sub>	8.53	9.90	9.08
Al <sub>2</sub> O <sub>3</sub>	0.13	0.47	0.19
FeO*	70.48	67.95	69.08
MgO	0.62	0.83	0.67
CaO	0.41	0.61	0.40
K <sub>2</sub> O	0.09	0.42	0.40
Total	80.26	80.18	79.82

Note: 1, dark red brown vesicle filling, Sample 483B-32-2, 116–123 cm; 2, bright red groundmass material, Sample 483B-32-2, 135–141 cm; 3, bright red vesicle filling, Sample 483B-32-2, 135–141 cm. Values shown in wt. %.

Table 11. Defocused microprobe analyses of smectites, Hole 485A.

Oxide	1	2	3	4	5	6	7	8	9
SiO <sub>2</sub>	43.91	41.27	44.64	45.92	44.32	40.08	44.30	45.10	44.47
TiO <sub>2</sub>	3.13	—	0.06	0.02	0.14	—	0.10	—	0.02
Al <sub>2</sub> O <sub>3</sub>	4.56	9.00	4.58	4.81	6.68	8.86	5.60	4.81	5.76
FeO*	12.96	14.17	12.48	16.25	15.33	15.08	15.33	13.80	14.79
MnO	0.16	0.19	0.10	0.09	0.09	0.05	0.08	—	0.11
MgO	16.59	17.41	17.55	16.95	16.93	14.90	16.49	17.45	17.13
CaO	1.75	1.44	1.50	1.77	2.00	2.00	1.86	1.60	1.55
Na <sub>2</sub> O	0.28	0.37	0.26	0.21	0.22	0.19	0.03	0.04	0.29
K <sub>2</sub> O	0.07	0.23	0.23	0.18	0.08	0.04	0.16	0.02	0.08
Total	83.41	84.08	81.40	86.20	85.79	79.73	83.95	82.82	84.20

Note: 1, smectite replacing clinopyroxene, Sample 485A-39-3, 49–54 cm; 2, brown smectite in groundmass, Sample 485A-39-3, 49–54 cm; 3, smectite pseudomorph after olivine, 485A-39-3, 49–54 cm; 4, brown smectite in groundmass, Sample 485A-39-3, 64–70 cm; 5, smectite pseudomorph after olivine, Sample 485A-39-3, 64–70 cm; 6–9, smectites in groundmass, Sample 485A-39-3, 64–70 cm. Values shown in wt. %.

trends. At any particular value of MgO, the glasses from Site 474 are richer in Al<sub>2</sub>O<sub>3</sub>, Na<sub>2</sub>O, K<sub>2</sub>O, and TiO<sub>2</sub> and poorer in total iron and CaO than the glasses from the other sites, reflecting their more alkalic nature. The single sample from Hole 477A is slightly offset from the 474A trend. With decreasing MgO, both groups show a regular decrease in CaO and Al<sub>2</sub>O<sub>3</sub> and an increase in total iron, Na<sub>2</sub>O, and TiO<sub>2</sub>. It is tempting to explain these variations by the co-precipitation of olivine and plagioclase. Saunders (this volume) has shown that much of the major element variation between the different basalt units from Sites 474, 482, and 483 could be explained by such a mechanism, but that since the incompatible element variations cannot be entirely reconciled in this way, open magma chamber fractional crystallization may have been involved. A hint of this is revealed by the lack of correlation between K<sub>2</sub>O and TiO<sub>2</sub> in Figure 3.

No such problems should be encountered, however, in comparing samples from the same eruptive unit. The two basalt samples from Hole 477A are both enriched in CaO and Al<sub>2</sub>O<sub>3</sub> and depleted in all of the other major elements relative to the glass sample. Similar variations are seen in several, but not all, of the basalt-glass pairs studied from Hole 474A. Since these basalts are plagioclase-

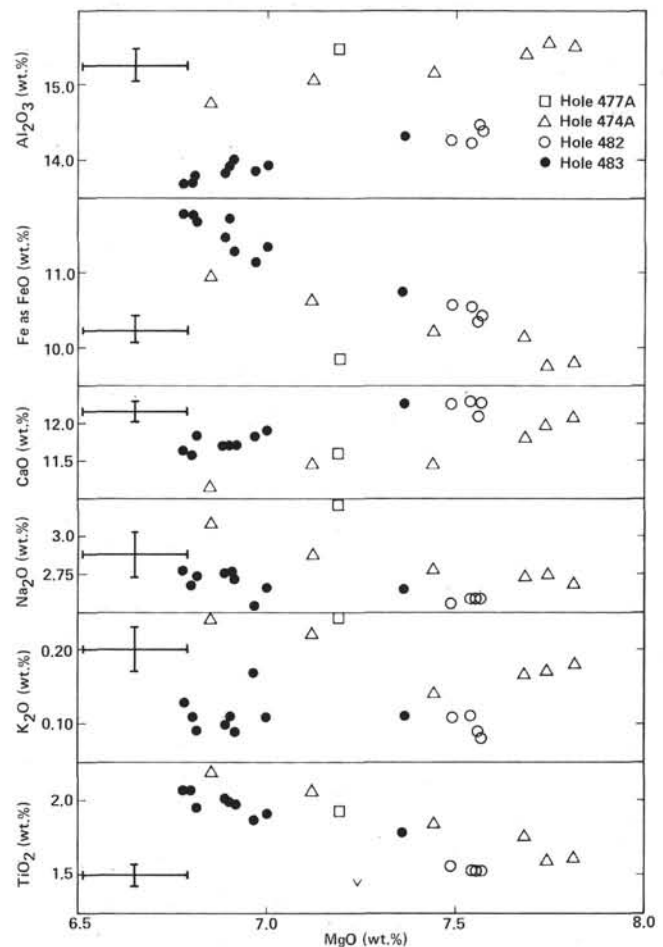


Figure 3. MgO variation diagram for glasses from Legs 64 and 65. (Error bars represent two standard deviations.)

class-phyric, the simplest way of explaining these differences is to postulate variable accumulation of plagioclase phenocrysts. Similar compositional differences between basalt-glass pairs have been reported by Thompson (1980) for plagioclase-phyric samples recovered during Legs 51 through 53. The intraunit chemical variation revealed by a comparison of the remaining glass and basalt samples is less easy to reconcile by means of any kind of fractionation model and indicates that metasomatic processes have also been involved.

Examination of Tables 12 and 13 shows that all of the basalt-glass pairs from Site 482 (Samples 482B-14-1, 115–118 cm; 482D-10-3, 81–85 cm; 482D-10-3, 106–110 cm; 482D-11-2, 70–74 cm; and Samples 482D-14-1, 90–94 cm; 482D-10-3, 130–135 cm; 482D-10-3, 130–135 cm; and 482D-11-2, 33–38 cm in Tables 12 and 13, respectively) show enrichment of the basalts in Al<sub>2</sub>O<sub>3</sub> and MgO and depletion in all of the other major elements, including CaO, relative to the glasses. The data could be explained if plagioclase fractionation was accompanied by high-temperature hydrothermal alteration. Some process involving plagioclase needs to be invoked to explain the Al<sub>2</sub>O<sub>3</sub> variations since this element is little affected by alteration at either high or low temperatures

Table 12. Analyses of basalts and standard reference sample, Legs 64 and 65.

	Sample (interval in cm)											
	474A-44-2, 65-67	474A-44-2, 128-130	474A-44-3, 34-38	474A-45-1, 82-83	474A-46-2, 25-27	474A-46-2, 28-30	474A-46-3, 81-82	474A-47-1, 86-88	474A-47-4, 38-40	474A-48-3, 28-39	474A-48-4, 88-90	474A-49-1, 141-143
Major elements (wt. %)												
SiO <sub>2</sub>	48.69	48.49	49.01	48.45	48.44	48.58	48.27	48.10	48.26	48.26	47.91	48.05
TiO <sub>2</sub>	1.80	1.86	1.81	1.75	1.41	1.44	1.43	1.32	1.34	1.52	1.69	1.79
Al <sub>2</sub> O <sub>3</sub>	16.54	16.03	16.58	15.69	17.26	17.14	16.45	17.69	18.13	16.66	19.84	16.62
Fe <sub>2</sub> O <sub>3</sub>	3.83	3.50	3.32	3.07	3.41	3.18	2.43	2.68	2.49	2.89	3.41	2.65
FeO	5.82	6.51	6.27	7.26	5.42	5.48	6.74	5.85	6.18	6.63	6.27	7.25
MnO	0.24	0.23	0.24	0.19	0.19	0.23	0.18	0.16	0.16	0.17	0.22	0.19
MgO	6.42	7.30	6.05	7.32	6.60	6.85	7.83	7.08	6.72	7.61	5.67	6.82
CaO	11.97	11.12	11.89	11.15	12.40	12.47	12.05	12.45	12.71	12.01	12.33	11.55
Na <sub>2</sub> O	2.77	2.88	3.05	2.73	2.56	2.62	2.55	2.42	2.42	2.56	2.55	2.71
K <sub>2</sub> O	0.07	0.09	0.11	0.14	0.08	0.08	0.11	0.08	0.08	0.09	0.15	0.14
P <sub>2</sub> O <sub>5</sub>	0.20	0.20	0.21	0.19	0.15	0.15	0.14	0.14	0.14	0.16	0.18	0.20
LOI <sup>a</sup>	1.44	1.80	1.63	1.77	1.77	1.72	1.36	1.67	1.42	1.38	1.58	1.54
Total	99.79	100.01	100.17	99.71	99.69	99.94	99.54	99.64	100.09	99.92	99.80	99.51
Trace elements (ppm)												
V	297	331	312	275	248	256	245	221	219	253	278	254
Cr	278	259	283	237	353	376	356	305	334	322	287	234
Co	50	53	53	42	43	50	49	42	43	43	43	46
Ni	97	99	98	82	117	117	123	97	107	102	97	88
Cu	59	65	63	57	57	63	59	53	52	58	49	45
Zn	85	79	86	71	69	68	72	64	66	69	81	74
Rb	nd	1	1	2	nd	nd	1	1	1	1	1	2
Sr	130	129	129	118	150	147	139	141	143	146	147	152
Y	51	52	52	49	39	37	38	34	35	39	43	43
Zr	128	136	130	131	92	97	98	91	90	106	121	130
Nb	6	7	3	7	3	8	6	3	3	4	8	8
Li	9	10	8	13	7	8	8	7	6	8	9	9
Sc	38	40	38	38	35	35	36	33	33	36	35	35

<sup>a</sup> Loss on ignition.

	Sample (interval in cm)												
	474A-49-2, 22-23	474A-50-2, 133-135	474A-50-3, 103-106	477A-1-1, 35-36	477A-1-1, 98-100	478-41-3, 40-42	478-41-3, 49-51	478-45-2, 36-36	478-45-2, 67-71	482B-10-7, 24-27	482B-10-7, 81-86	482B-11-2, 87-91	482B-12-1, 32-36
Major elements (wt. %)													
SiO <sub>2</sub>	48.07	48.36	48.70	48.68	48.17	48.00	47.90	50.14	47.96	47.12	49.31	49.78	47.77
TiO <sub>2</sub>	1.76	2.19	2.17	1.59	1.58	1.37	1.23	1.54	1.27	1.85	1.73	1.73	1.49
Al <sub>2</sub> O <sub>3</sub>	17.06	15.11	14.75	17.13	17.32	15.56	16.29	14.74	15.99	15.12	14.32	14.18	14.41
Fe <sub>2</sub> O <sub>3</sub>	5.03	5.79	4.14	9.64	9.51	2.38	1.77	3.26	2.35	11.05	1.20	3.13	10.99
FeO	4.95	5.17	7.49	—	—	6.22	6.28	6.15	5.83	—	8.31	7.52	—
MnO	0.18	0.19	0.20	0.18	0.17	0.16	0.18	0.19	0.18	0.23	0.23	0.19	0.17
MgO	6.19	8.22	6.41	6.92	6.49	7.61	8.15	6.86	8.04	6.98	7.43	7.48	8.77
CaO	11.79	7.92	10.95	11.97	12.06	10.72	10.75	11.65	11.27	9.81	12.01	11.89	9.49
Na <sub>2</sub> O	2.77	3.07	2.96	2.85	3.00	3.76	3.65	3.13	3.08	3.01	2.69	2.60	3.07
K <sub>2</sub> O	0.13	0.16	0.14	0.15	0.16	0.30	0.29	0.33	0.20	0.07	0.08	0.09	0.13
P <sub>2</sub> O <sub>5</sub>	0.20	0.23	0.23	0.19	0.19	0.16	0.14	0.20	0.14	0.18	0.18	0.17	0.14
LOI <sup>a</sup>	1.24	2.70	1.48	0.56	0.77	3.49	3.38	1.70	3.62	4.05	1.72	1.20	2.86
Total	99.37	99.11	99.62	99.86	99.42	99.73	100.01	99.89	99.93	99.47	99.21	99.96	99.29
Trace elements (ppm)													
V	268	373	315	220	210	180	168	217	168	346	327	293	318
Cr	246	231	227	239	229	252	255	306	269	287	382	252	314
Co	43	51	35	39	40	45	41	41	40	44	45	37	40
Ni	85	69	72	75	69	82	101	53	99	67	66	58	71
Cu	49	59	55	59	56	61	50	61	49	65	63	55	49
Zn	79	84	82	62	59	51	54	59	54	77	76	65	69
Rb	nd	1	1	nd	nd	4	4	3	4	nd	nd	nd	nd
Sr	147	153	150	231	240	175	186	199	215	112	113	142	100
Y	44	55	57	36	34	31	29	39	29	48	50	51	44
Zr	122	150	150	123	119	103	92	125	92	115	115	116	95
Nb	7	7	7	6	4	2	2	2	4	3	3	1	3
Li	8	9	9	7	6	5	5	6	7	8	10	10	8
Sc	35	40	41	35	35	37	34	43	36	47	44	44	43

(Humphris and Thompson, 1978; Humphris et al., 1980). High-temperature alteration of the basalts would both increase the MgO content and decrease the CaO content. Similar variations are shown by one of the basalt-glass pairs from Hole 474A (Samples 474A-46-3, 81-82 and 474A-46-2, 111-114 in Tables 12 and 13, respectively).

### Intraunit Variations

Samples of fresh glass were only available from a few of the cooling units. In the case of the other samples, most of which were from massive units, the nature of the chemical trends during alteration can only be determined by comparing samples from the same unit

Table 12. (Continued).

	Sample (interval in cm)											
	482B-12-2, 105-108	482B-14-1, 115-118	482B-14-2, 136-140	482B-19-1, 66-70	482B-20-1, 30-33	482B-21-3, 65-68	482B-22-2, 39-43	482B-22-2, 53-57	482B-22-4, 19-22	482C-10-1, 13-14	482C-10-1, 89-92	482C-10-1, 114-117
Major elements (wt.%)												
SiO <sub>2</sub>	48.34	49.44	49.61	49.30	49.30	49.51	49.69	49.64	49.72	48.43	49.55	49.51
TiO <sub>2</sub>	1.69	1.39	1.40	1.95	1.86	1.61	1.55	1.60	1.52	1.82	1.80	1.80
Al <sub>2</sub> O <sub>3</sub>	13.83	14.82	14.95	14.40	15.01	15.59	15.49	16.39	15.11	14.41	14.30	14.17
Fe <sub>2</sub> O <sub>3</sub>	2.68	2.76	2.65	3.93	4.15	3.45	3.13	3.37	3.43	11.19	3.26	3.38
FeO	7.66	7.72	7.70	7.97	6.79	6.61	6.96	5.77	6.40	—	7.39	7.40
MnO	0.19	0.20	0.20	0.20	0.15	0.20	0.18	0.15	0.16	0.22	0.21	0.20
MgO	7.62	7.85	7.90	7.73	7.74	7.31	7.12	7.16	7.86	8.21	7.75	7.70
CaO	11.28	11.98	12.03	10.00	10.75	11.86	12.02	11.44	11.72	11.06	11.32	11.38
Na <sub>2</sub> O	2.40	2.45	2.45	2.88	2.82	2.62	2.68	2.75	2.58	2.33	2.58	2.59
K <sub>2</sub> O	0.08	0.09	0.07	0.06	0.05	0.04	0.04	0.05	0.07	0.10	0.08	0.09
P <sub>2</sub> O <sub>5</sub>	0.17	0.13	0.13	0.19	0.19	0.16	0.15	0.15	0.15	0.17	0.18	0.17
LOI <sup>a</sup>	3.81	1.18	1.16	1.46	1.33	1.08	0.95	1.28	1.37	1.77	1.12	1.15
Total	99.75	100.01	100.25	100.07	100.14	100.04	99.96	99.75	100.09	99.71	99.54	99.54
Trace elements (ppm)												
V	285	135	135	181	360	287	279	314	276	337	310	—
Cr	256	267	268	114	119	210	215	226	276	258	265	—
Co	38	44	48	45	49	44	41	46	44	43	44	—
Ni	62	87	94	45	50	58	51	60	85	63	65	—
Cu	59	70	65	64	63	60	58	64	64	62	67	—
Zn	65	78	78	93	79	70	69	68	67	78	71	—
Rb	nd	1	1	1	nd	1	nd	nd	nd	1	1	—
Sr	105	92	103	102	92	130	124	132	126	104	105	—
Y	50	39	56	60	42	47	42	43	42	48	49	—
Zr	113	85	79	134	130	110	109	109	100	115	121	—
Nb	3	3	4	3	2	2	4	2	5	3	3	—
Li	8	7	7	8	8	8	7	7	9	7	6	6
Sc	42	40	41	45	47	42	42	43	43	47	44	43

	Sample (interval in cm)											
	482C-10-2, 96-100	482C-10-3, 51-55	482C-11-1, 24-29	482C-11-1, 101-105	482C-11-2, 71-75	482C-11-4, 98-102	482C-12-1, 0-5	482C-12-1, 92-118	482C-12-2, 8-15	482D-10-3, 81-85	482D-10-3, 106-110	482D-11-2, 70-74
Major elements (wt.%)												
SiO <sub>2</sub>	49.55	49.56	49.51	49.80	49.31	49.84	50.25	50.11	50.30	49.41	49.49	49.43
TiO <sub>2</sub>	1.72	1.69	1.72	1.56	1.49	1.75	1.29	1.26	1.27	1.45	1.38	1.38
Al <sub>2</sub> O <sub>3</sub>	14.28	14.20	14.56	14.45	14.14	14.10	14.65	14.59	14.70	15.39	14.82	14.86
Fe <sub>2</sub> O <sub>3</sub>	3.38	3.22	3.81	3.31	4.04	3.25	2.99	2.90	2.94	3.10	2.83	3.01
FeO	7.07	7.09	6.33	6.76	6.55	7.75	7.34	7.27	7.02	6.65	7.34	7.16
MnO	0.20	0.17	0.16	0.19	0.15	0.19	0.17	0.16	0.18	0.19	0.19	0.19
MgO	7.94	7.85	8.06	8.54	9.03	8.00	7.98	7.76	7.90	7.51	7.78	7.78
CaO	11.55	11.74	11.46	10.29	10.62	11.18	11.69	12.06	12.03	11.33	11.99	12.02
Na <sub>2</sub> O	2.64	2.59	2.76	3.12	2.67	2.56	2.47	2.37	2.38	2.61	2.44	2.44
K <sub>2</sub> O	0.07	0.07	0.08	0.14	0.07	0.08	0.06	0.06	0.07	0.06	0.06	0.06
P <sub>2</sub> O <sub>5</sub>	0.17	0.16	0.17	0.17	0.15	0.17	0.12	0.12	0.12	0.13	0.13	0.13
LOI <sup>a</sup>	1.32	1.25	1.27	1.82	1.79	1.34	1.05	1.16	1.07	1.82	1.44	1.38
Total	99.89	99.59	99.89	100.15	100.01	100.21	100.06	99.82	99.98	99.65	99.90	99.78
Trace elements (ppm)												
V	296	285	314	281	295	300	290	280	268	297	269	264
Cr	241	260	256	280	284	261	181	185	151	288	274	258
Co	41	41	48	47	46	43	42	48	47	49	44	50
Ni	63	62	68	71	70	62	51	51	49	93	91	85
Cu	57	52	47	32	110	54	64	69	67	72	60	62
Zn	64	64	59	61	49	64	68	68	65	80	77	72
Rb	nd	nd	nd	3	1	nd	nd	1	1	1	1	nd
Sr	107	125	112	103	101	108	89	90	94	93	91	98
Y	47	47	48	47	42	52	38	37	39	44	39	39
Zr	115	109	113	104	85	114	75	72	70	86	82	80
Nb	3	nd	nd	3	1	2	1	nd	2	1	nd	2
Li	7	6	6	12	8	10	7	8	8	6	—	7
Sc	43	42	44	41	41	38	41	40	41	42	—	40

which show different degrees of alteration. Figure 4 shows selected minor and trace element data plotted against Zr for flows or sills from which multiple samples were collected. Examination of this figure shows that many of these units have been affected by considerable amounts of *in situ* fractional crystallization. This is

clearly demonstrated by the covariation shown by Y, Zr, and TiO<sub>2</sub> in virtually all cases, since these elements are normally incompatible in basaltic liquids. The lack of correlation in several units between Sr and K<sub>2</sub>O on the one hand and these elements on the other clearly suggests that Sr and K<sub>2</sub>O were mobile, though the na-

Table 12. (Continued).

	Sample (interval in cm)											
	482D-11-3, 74-78	483-15-1, 90-93	483-15-2, 40-45	483-22-4, 54-58	483-25-1, 71-79	483-25-1, 85-90	483-25-2, 14-20	483-26-2, 31-37	483-26-2, 68-74	483-26-2, 83-88	483B-8-1, 62-66	483B-8-1, 137-143
Major elements (wt.%)												
SiO <sub>2</sub>	49.43	49.76	49.70	49.30	49.42	49.38	49.00	48.57	49.22	49.20	48.34	48.50
TiO <sub>2</sub>	1.39	1.21	1.20	1.72	2.21	2.09	2.06	2.08	2.12	2.13	0.95	0.95
Al <sub>2</sub> O <sub>3</sub>	14.96	14.97	14.86	15.99	14.52	13.94	13.67	14.13	14.03	14.13	16.41	16.52
Fe <sub>2</sub> O <sub>3</sub>	2.99	3.03	2.79	3.35	3.89	3.31	3.71	4.13	3.86	3.93	1.94	2.56
FeO	7.26	6.22	6.76	6.40	7.35	8.66	8.05	7.89	8.24	7.92	6.78	6.14
MnO	0.21	0.18	0.19	0.22	0.18	0.21	0.19	0.21	0.23	0.21	0.17	0.16
MgO	7.66	7.83	8.45	6.93	7.06	6.95	7.19	7.04	6.66	6.81	9.45	9.04
CaO	12.04	12.42	12.43	11.63	11.00	11.11	11.25	11.37	11.25	11.08	12.16	12.29
Na <sub>2</sub> O	2.44	2.63	2.58	2.65	2.89	2.65	2.73	2.54	2.69	2.66	2.32	2.23
K <sub>2</sub> O	0.06	0.07	0.08	0.09	0.11	0.07	0.11	0.07	0.11	0.08	0.04	0.05
P <sub>2</sub> O <sub>5</sub>	0.13	0.11	0.11	0.17	0.22	0.21	0.20	0.21	0.21	0.22	0.08	0.09
LOI <sup>a</sup>	1.54	1.29	1.15	1.16	1.31	1.22	1.48	1.50	1.52	1.47	1.83	1.93
Total	100.11	99.72	100.29	99.61	100.16	99.80	99.64	99.74	100.14	99.84	100.47	100.46
Trace elements (ppm)												
V	281	238	224	316	378	—	297	346	346	357	179	179
Cr	257	328	343	300	147	—	137	145	153	162	324	320
Co	47	44	38	49	44	—	43	45	46	45	53	50
Ni	82	58	56	88	71	—	64	66	64	63	100	100
Cu	62	64	71	66	56	—	48	53	53	54	86	86
Zn	75	55	60	85	92	—	79	91	91	93	53	57
Rb	1	1	nd	1	1	—	1	1	1	1	nd	nd
Sr	94	116	114	108	116	—	129	107	105	107	92	97
Y	44	32	33	51	62	—	60	58	59	61	26	29
Zr	79	68	63	117	154	—	142	143	147	148	47	54
Nb	2	1	nd	3	3	—	2	2	1	5	1	nd
Li	8	9	8	9	12	11	12	10	10	13	—	8
Sc	41	43	43	43	44	42	41	41	42	42	—	35

	Sample (interval in cm)											
	483B-8-2, 134-141	483B-8-3, 2-20	483B-18-1, 27-31	483B-18-1, 67-70	483B-18-1, 43-97	483B-18-1, 140-144	483B-18-2, 6-11	483B-25-2, 22-28	483B-25-2, 69-73	483B-25-2, 110-117	483B-25-2, 122-128	483B-32-2, 116-123
Major elements (wt.%)												
SiO <sub>2</sub>	48.00	47.90	48.57	48.84	49.34	48.48	47.93	48.74	47.94	48.83	48.81	49.27
TiO <sub>2</sub>	0.95	1.04	2.11	2.12	2.10	2.20	2.13	2.01	1.75	1.96	1.72	1.58
Al <sub>2</sub> O <sub>3</sub>	16.38	16.27	14.22	13.84	13.90	14.41	13.85	15.21	14.36	15.23	14.51	15.18
Fe <sub>2</sub> O <sub>3</sub>	2.44	2.60	4.16	4.32	4.43	4.62	3.95	4.30	4.83	3.28	5.04	4.57
FeO	6.13	6.35	7.28	7.81	7.48	6.69	8.06	6.38	6.69	7.26	6.65	5.82
MnO	0.16	0.17	0.21	0.21	0.20	0.20	0.22	0.20	0.23	0.20	0.24	0.22
MgO	8.95	9.09	7.27	7.28	7.30	7.36	7.19	6.83	7.06	6.85	7.24	7.51
CaO	12.19	11.98	10.76	10.43	10.41	10.76	10.82	11.01	10.38	11.53	10.91	11.56
Na <sub>2</sub> O	2.29	2.09	2.89	2.74	2.58	2.88	2.76	2.93	2.72	2.90	2.61	2.54
K <sub>2</sub> O	0.05	0.05	0.09	0.22	0.10	0.09	0.25	0.08	0.44	0.08	0.26	0.21
P <sub>2</sub> O <sub>5</sub>	0.09	0.09	0.22	0.22	0.21	0.23	0.23	0.19	0.17	0.19	0.17	0.16
LOI <sup>a</sup>	2.45	2.56	1.59	1.80	1.57	2.01	2.36	1.96	2.85	1.69	1.77	1.30
Total	100.08	99.48	99.37	99.83	99.92	99.93	99.75	99.84	99.42	100.00	99.93	99.92
Trace elements (ppm)												
V	174	206	374	349	332	388	392	379	344	364	309	305
Cr	279	305	160	138	135	149	148	167	145	139	135	320
Co	57	52	46	41	47	53	45	59	50	50	30	48
Ni	103	109	63	61	57	61	63	65	71	61	44	96
Cu	83	79	46	51	50	53	56	62	59	63	47	60
Zn	57	62	87	82	82	93	86	93	71	93	78	74
Rb	nd	1	1	4	1	1	4	nd	8	nd	7	4
Sr	160	134	108	107	109	112	111	123	113	122	109	117
Y	27	30	61	62	60	62	65	55	48	53	47	44
Zr	51	59	146	145	147	155	149	126	106	123	101	95
Nb	3	3	2	2	3	6	6	nd	1	1	2	2
Li	13	9	11	11	—	12	12	11	10	11	14	8
Sc	33	33	43	41	—	42	40	42	37	41	38	41

ture of the trends is virtually impossible to quantify. Trends such as those shown in Figure 4 could in theory be the result of extensive alteration since this can cause changes in the abundances but not the ratios of relatively immobile elements. Several considerations argue against this hypothesis, however: First, the negative cor-

relation shown by Ni and Zr in several of the units could easily be the result of fractionation or accumulation of olivine but could never be the result of the minor amounts of alteration shown by most of these samples; second, the fact that the most extensive variations are shown by the most massive units, such as the sills or

Table 12. (Continued).

	Sample (interval in cm)											
	483B-32-2, 135-141	483B-28-1, 42-59	485A-24-1, 42-47	485A-24-1, 69-73	485A-25-1, 117-143	485A-30-2, 4-10	485A-30-2, 50-56	485A-30-3, 31-37	485A-30-3, 49-54	485A-30-3, 138-142	485A-31-1, 76-80	485A-34-1, 90-95
Major elements (wt.%)												
SiO <sub>2</sub>	49.44	49.14	49.43	49.14	48.99	49.40	49.95	49.18	49.50	49.61	49.14	49.72
TiO <sub>2</sub>	1.57	1.75	2.06	2.14	2.11	2.56	2.75	1.84	1.91	1.79	1.64	1.84
Al <sub>2</sub> O <sub>3</sub>	14.81	14.06	14.93	15.14	14.47	12.65	12.78	14.17	14.30	14.61	14.15	14.35
Fe <sub>2</sub> O <sub>3</sub>	3.15	3.28	3.64	4.31	3.20	4.05	4.15	3.63	3.59	2.82	3.01	3.82
FeO	6.73	7.79	7.01	6.31	8.42	9.22	8.22	6.90	6.43	7.16	7.38	6.92
MnO	0.22	0.22	0.20	0.18	0.21	0.24	0.19	0.17	0.19	0.20	0.22	0.17
MgO	7.88	7.63	7.13	7.40	7.19	7.12	7.34	7.74	8.17	7.59	8.45	7.53
CaO	12.01	11.36	11.18	10.52	11.02	10.32	10.18	11.66	11.10	11.77	12.11	10.88
Na <sub>2</sub> O	2.54	2.53	2.95	2.79	2.49	2.76	2.87	2.46	2.73	2.54	2.22	2.68
K <sub>2</sub> O	0.10	0.10	0.10	0.07	0.08	0.08	0.06	0.08	0.07	0.08	0.13	0.07
P <sub>2</sub> O <sub>5</sub>	0.15	0.17	0.20	0.21	0.21	0.24	0.26	0.18	0.16	0.17	0.15	0.17
LOI <sup>a</sup>	1.22	1.61	1.22	1.37	1.37	1.35	1.40	1.45	1.70	1.42	1.28	1.52
Total	99.82	99.64	100.05	99.58	99.76	99.99	100.15	99.46	99.85	99.76	99.88	99.67
Trace elements (ppm)												
V	284	324	374	398	351	371	413	308	340	291	270	327
Cr	303	217	191	200	205	175	132	469	367	401	380	245
Co	47	49	45	50	42	42	36	40	32	43	40	46
Ni	120	73	79	87	71	43	45	79	72	80	99	65
Cu	64	57	27	43	45	46	14	64	10	40	42	55
Zn	77	78	76	77	85	83	62	61	50	61	78	73
Rb	2	nd	nd	nd	1	1	2	2	nd	1	3	1
Sr	118	105	115	121	104	108	112	103	104	108	99	107
Y	42	49	59	59	61	77	80	49	51	53	49	50
Zr	96	106	134	140	136	166	187	113	107	113	95	116
Nb	4	2	nd	3	2	2	3	1	4	3	1	nd
Li	9	11	12	14	12	15	13	12	16	12	12	10
Sc	41	44	43	45	42	48	48	45	44	43	43	44

	Sample (interval in cm)					Standard Reference Sample (BOB-1)					
	485A-39-1, 4-10	485A-39-1, 16-22	485A-39-1, 68-72	485A-39-1, 119-124	485A-39-3, 4-70	1	2	3	4	Mean	
Major elements (wt.%)											
SiO <sub>2</sub>	48.99	49.63	49.51	49.41	49.15	SiO <sub>2</sub>	50.57	50.52	50.67	50.31	50.52
TiO <sub>2</sub>	1.69	1.95	2.07	2.19	2.04	TiO <sub>2</sub>	1.27	1.26	1.26	1.27	1.27
Al <sub>2</sub> O <sub>3</sub>	14.89	14.32	13.96	12.95	14.71	Al <sub>2</sub> O <sub>3</sub>	16.64	16.56	16.44	16.56	16.55
Fe <sub>2</sub> O <sub>3</sub>	3.30	3.25	3.82	3.01	3.87	FeO*	8.39	8.40	8.36	8.42	8.39
FeO	7.28	7.95	7.84	9.29	8.02	MnO	0.15	0.16	0.16	0.14	0.15
MnO	0.20	0.19	0.22	0.24	0.19	MgO	7.58	7.49	7.62	7.65	7.59
MgO	8.00	7.32	7.12	7.57	6.61	CaO	11.17	11.23	11.20	11.19	11.20
CaO	11.15	11.25	11.32	11.27	10.75	Na <sub>2</sub> O	2.94	3.39	3.17	2.99	3.12
Na <sub>2</sub> O	2.50	2.52	2.59	2.57	2.63	K <sub>2</sub> O	0.38	0.40	0.37	0.38	0.38
K <sub>2</sub> O	0.07	0.06	0.06	0.07	0.06	P <sub>2</sub> O <sub>5</sub>	0.17	0.18	0.17	0.17	0.17
P <sub>2</sub> O <sub>5</sub>	0.16	0.19	0.19	0.20	0.20	LOI	0.68	0.68	0.68	0.68	0.68
LOI <sup>a</sup>	1.62	1.40	1.15	1.29	1.47	Total	99.94	100.27	100.10	99.76	100.02
Total	99.85	100.03	99.85	100.06	99.70						
Trace elements (ppm)											
V	304	343	340	373	338	V	211	223	221	218	218.3
Cr	220	214	199	226	113	Cr	299	294	299	287	294.8
Co	50	38	44	43	45	Co	60	65	65	64	63.5
Ni	98	67	61	50	81	Ni	103	103	109	106	105.3
Cu	49	53	57	44	46	Cu	59	58	60	58	58.8
Zn	70	75	76	79	79	Zn	64	63	63	78	67.0
Rb	1	1	nd	1	1	Rb	6	4	6	6	5.5
Sr	104	103	104	101	126	Sr	190	195	196	195	194.0
Y	49	55	59	60	57	Y	32	33	32	34	32.8
Zr	107	124	131	132	126	Zr	98	99	99	102	99.5
Nb	4	3	2	5	3	Nb	5	7	7	3	5.5
Li	12	11	9	11	10	Li	2	nd	nd	1	—
Sc	40	44	45	48	39	Sc	31	16	nd	nd	—

flows from Holes 478 and 485A, and the tendency for the data from several units at one site to line up along the same trend, clearly support a fractionation mechanism.

Figure 4 was used to select those units which show little or no *in situ* fractionation. After rejecting those

which also showed little or no variation in the degree of alteration, the CaO, MgO, and K<sub>2</sub>O contents of the resultant, very reduced sample set were plotted against loss on ignition as an index of alteration in an attempt to identify the processes responsible for the variations. Although several altered samples were thus excluded from

Table 13. Microprobe analyses of glasses, Legs 64 and 65.

Oxide	Sample (interval in cm)									
	477A-1-1, 1-3	474A-44-3, 34-38	474A-46-2, 111-114	474A-47-4, 69-71	474A-48-3, 1-2	474A-48-4, 82-83	474A-49-1, 1-6	482B-14-1, 90-94	482D-10-3, 81-85	
SiO <sub>2</sub>	50.11	50.43	49.75	49.95	49.67	49.96	50.09	50.76	50.59	
Al <sub>2</sub> O <sub>3</sub>	15.48	15.15	15.52	15.55	15.41	15.02	14.71	14.45	14.20	
Cr <sub>2</sub> O <sub>3</sub>	—	0.07	0.08	0.06	0.07	0.08	0.08	—	0.10	
FeO*	9.84	10.23	9.86	9.75	10.16	10.64	10.96	10.29	10.53	
MnO	0.16	0.19	0.18	0.19	0.22	0.16	0.21	0.18	0.20	
MgO	7.19	7.44	7.81	7.74	7.68	7.12	6.85	7.56	7.54	
NiO	—	—	—	—	—	—	—	—	—	
CaO	11.58	11.46	12.09	11.97	11.80	11.49	11.14	12.09	12.29	
Na <sub>2</sub> O	3.22	2.77	2.68	2.74	2.73	2.88	3.09	2.58	2.57	
K <sub>2</sub> O	0.24	0.14	0.18	0.17	0.17	0.22	0.24	0.09	0.11	
TiO <sub>2</sub>	1.92	1.84	1.61	1.59	1.76	2.05	2.18	1.52	1.52	
P <sub>2</sub> O <sub>5</sub>	0.07	0.14	0.09	0.12	—	0.11	0.16	—	0.21	
Total	99.81	99.86	99.85	99.83	99.67	99.73	99.71	99.52	99.86	

Note: Each analysis listed represents a mean of 10 separate analyses. Values shown in wt. %.

the data set, the results should still be typical of most of the basalts because the secondary minerals at any one site are similar in composition (Fig. 2). The results of this exercise are shown in Figures 5 through 7. For purposes of comparison, the changes shown by Humphris and G. Thompson (1978) across individual pillows subjected to hydrothermal alteration and the variations produced during typical low-temperature alteration of basalts by seawater (Pritchard et al., 1979) were also plotted in the upper and lower right-hand diagrams, respectively, of Figures 5, 6, and 7.

Figures 5 through 7 clearly demonstrate that the variations shown by the basalts from Sites 474 and 482 closely resemble those generated during high-temperature hydrothermal alteration of basalts by seawater—i.e., a loss of CaO, increases in MgO, and little or no change in K<sub>2</sub>O. In contrast, the basalts from Site 483 show little or no systematic change in their CaO and MgO contents as a result of increasing hydration, but do show large variations in their K<sub>2</sub>O contents—variations typical of low-temperature alteration. It seems likely that the samples from Site 485 were also affected by hydrothermal alteration in view of the many similarities in secondary minerals formed at Sites 474, 482, and 485.

### CONCLUSIONS

The best way of explaining the findings outlined in this chapter is to postulate that short-lived hydrothermal systems exist near the crest of the East Pacific Rise and have existed in this region in the past. The layer-cake nature of the oceanic crust in this area, i.e. interdigitated, laterally extensive layers of relatively impermeable sediments and more permeable basalts, make it very unlikely that the fluids in these systems would have penetrated more than a few basalt units at any one time. The hydrothermal vein in the upper unit in Hole 482C may well have been a vent for one of these small systems. Significantly, although Moorby et al. (this volume) could find little evidence of Fe-enriched basal sediments in this region of the type found elsewhere along the East Pacific Rise and Rise flanks, they did suggest

that some hydrothermally derived sulfide material may have been added to the sediments at Site 482.

The high sedimentation rates in the mouth of the Gulf of California will cause any such systems to be very short-lived, since fluid channels will be rapidly choked by the influx of detrital material. Until the crust moves away from the active spreading center and cools, some circulation will still occur but the blanketing effect of the overlying sediments will preclude any significant exchange with the seawater. Instead, the fluid compositions will probably be buffered by the basalts, causing the samples to retain a chemical fingerprint of the hydrothermal alteration which took place, even though the greenschist-facies minerals will be gradually replaced by species stable at lower temperatures.

The differences in the alteration mineralogy between Site 483 and the other sites examined on Legs 64 and 65 can thus be explained by the lower sedimentation rate at Site 483, which allowed seawater to have access to the basalt for a longer period of time. Although the sedimentation rate at Site 483 is high compared to that at most other oceanic spreading centers, the sediment accumulation rates at the other sites investigated here were an order of magnitude higher.

### ACKNOWLEDGMENTS

We would like to thank the Leg 64 shipboard scientific party for collecting samples from the core on our behalf. Considerable thanks are also due to P. Suddaby and N. Wilkinson for their efforts in maintaining the Imperial College microprobe system in peak operating condition and to P. Watkins for performing the FeO analyses. This work was supported by the N.E.R.C. through Grant GR3/2946. The EDS detector was provided by the N.E.R.C. through Grant GR3/3357. The manuscript was improved as a result of critical comments from G. L. Hendry.

### REFERENCES

- Bass, M. N., 1976. Secondary minerals in oceanic basalt, with special reference to Leg 34, DSDP. In Yeats, R. S., Hart, S. R., et al., *Init. Repts. DSDP*, 34: Washington (U.S. Govt. Printing Office), 393-432.
- Boström, K., and Peterson, M. N. A., 1966. Precipitates from hydrothermal exhalations on the East Pacific Rise. *Econ. Geol.*, 61: 1285-1265.

Table 13. (Continued).

Sample (interval in cm)										
482D-10-3, 130-135	482D-11-2, 33-38	483-20-1, 105-109	483-21-3, 47-51	483-22-1, 2-7	483-22-1, 65-68	483B-13-2, 48-53	483B-23-1, 79-84	483B-23-1, 112-116	483B-30-2, 37-43	483B-32-2, 90-95
50.59	50.50	50.40	51.01	50.65	50.37	50.35	50.14	50.25	50.45	50.33
14.38	14.25	13.67	14.00	13.81	13.92	13.69	13.88	13.79	13.82	14.29
—	0.10	0.10	0.08	—	—	—	0.04	—	—	0.05
10.43	10.56	11.77	11.28	11.11	11.32	11.76	11.72	11.66	11.44	10.74
0.16	0.16	0.22	0.19	0.20	0.19	0.21	0.26	0.23	0.22	0.17
7.57	7.49	6.78	6.91	6.97	7.01	6.80	6.90	6.81	6.89	7.36
—	—	—	—	—	—	—	—	—	—	0.02
12.27	12.25	11.63	11.46	11.82	11.87	11.57	11.70	11.83	11.72	12.26
2.59	2.54	2.77	2.72	2.56	2.66	2.68	2.76	2.73	2.76	2.65
0.08	0.11	0.13	0.09	0.17	0.11	0.11	0.11	0.09	0.10	0.11
1.53	1.55	2.06	1.97	1.86	1.91	2.06	1.98	1.95	2.00	1.77
0.16	0.17	0.19	0.11	0.33	0.21	0.20	0.15	0.12	0.15	0.12
99.76	99.68	99.72	99.82	99.48	99.57	99.43	99.64	99.46	99.55	99.87

- Duennebier, F., and Blackinton, G., 1980. A man-made hot spring on the ocean floor. *Nature*, 284:338-340.
- Einsele, G., Gieskes, J. M., Curray, J., et al., 1980. Intrusion of basaltic sills into highly porous sediments and resulting hydrothermal activity. *Nature*, 283:441-445.
- Flower, M. F. J., Ohnmacht, W., Schminke, H.-U., et al., 1978. Petrology and geochemistry of basalts from Hole 396B, Leg 46. In Dmitriev, L., Heirtzler, J., et al., *Init. Repts. DSDP*, 46: Washington (U.S. Govt. Printing Office), 179-213.
- Haymon, R. M., and Kastner, M., 1981. Hot spring deposits on the East Pacific Rise at 21°N: Preliminary description of mineralogy and genesis. *Earth Planet. Sci. Lett.*, 53:363-381.
- Humphris, S. E., Melson, W. G., and Thompson, R. N., 1980. Basalt weathering on the East Pacific Rise and the Galapagos Spreading Center, Deep Sea Drilling Project Leg 54. In Rosendahl, B. R., Hekinian, R., et al., *Init. Repts. DSDP*, 54: Washington (U.S. Govt. Printing Office), 773-787.
- Humphris, S. E., and Thompson, G., 1978. Hydrothermal alteration of oceanic basalts by seawater. *Geochim. Cosmochim. Acta*, 42: 107-125.
- Pritchard, R. G., Cann, J. R., and Wood, D. A., 1979. Low-temperature alteration of oceanic basalts, DSDP Leg 49. In Luyendyk, B. P., Cann, J. R., et al., *Init. Repts. DSDP*, 49: Washington (U.S. Govt. Printing Office), 709-714.
- Robinson, P. T., Flower, M. F. J., Schminke, H.-U., et al., 1977. Low temperature alteration of oceanic basalts, DSDP Leg 37. In Aumento, F., Melson, W. G., et al., *Init. Repts. DSDP*, 37: Washington (U.S. Govt. Printing Office), 775-794.
- Scarfe, C. M., and Smith, D. G. W., 1977. Secondary minerals in some basaltic rocks from DSDP Leg 37. *Can. J. Earth Sci.*, 14:903-910.
- Thompson, R. N., 1980. Major-element chemistry of basaltic glasses in Hole 418A lavas and a dyke: Deep Sea Drilling Project Legs 52 and 53. In Donnelly, T., Francheteau, J., Bryan, W., Robinson, P., Flower, M., Salisbury, M., et al., *Init. Repts. DSDP*, 51, 53, Pt. 2 Washington (U.S. Govt. Printing Office), 973-976.
- Walsh, J. N., 1980. The simultaneous determination of the major, minor and trace constituents of silicate rocks using inductively coupled plasma spectrometry. *Spectrochimica Acta*, 35B:107-111.
- Whipple, E. R., 1974. A study of Watson's determination of ferrous ion, in silicates. *Chem. Geol.*, 14:223-238.
- Wolery, T. J., and Sleep, N. H., 1976. Hydrothermal circulation and geochemical flux at mid-ocean ridges. *J. Geol.*, 84:249-275.

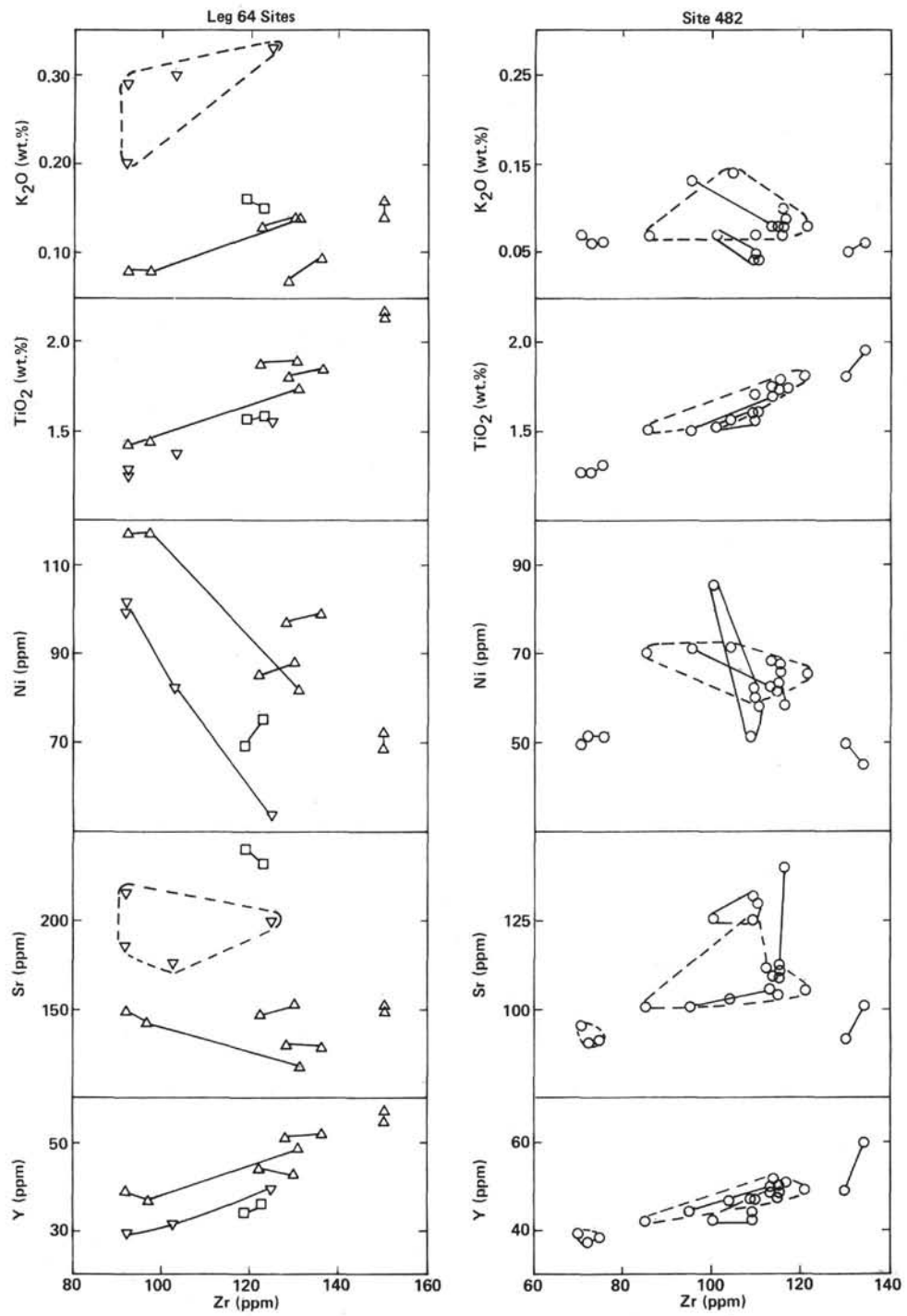


Figure 4. Variation of selected minor and trace elements versus Zr within basalt units drilled on Legs 64 and 65.

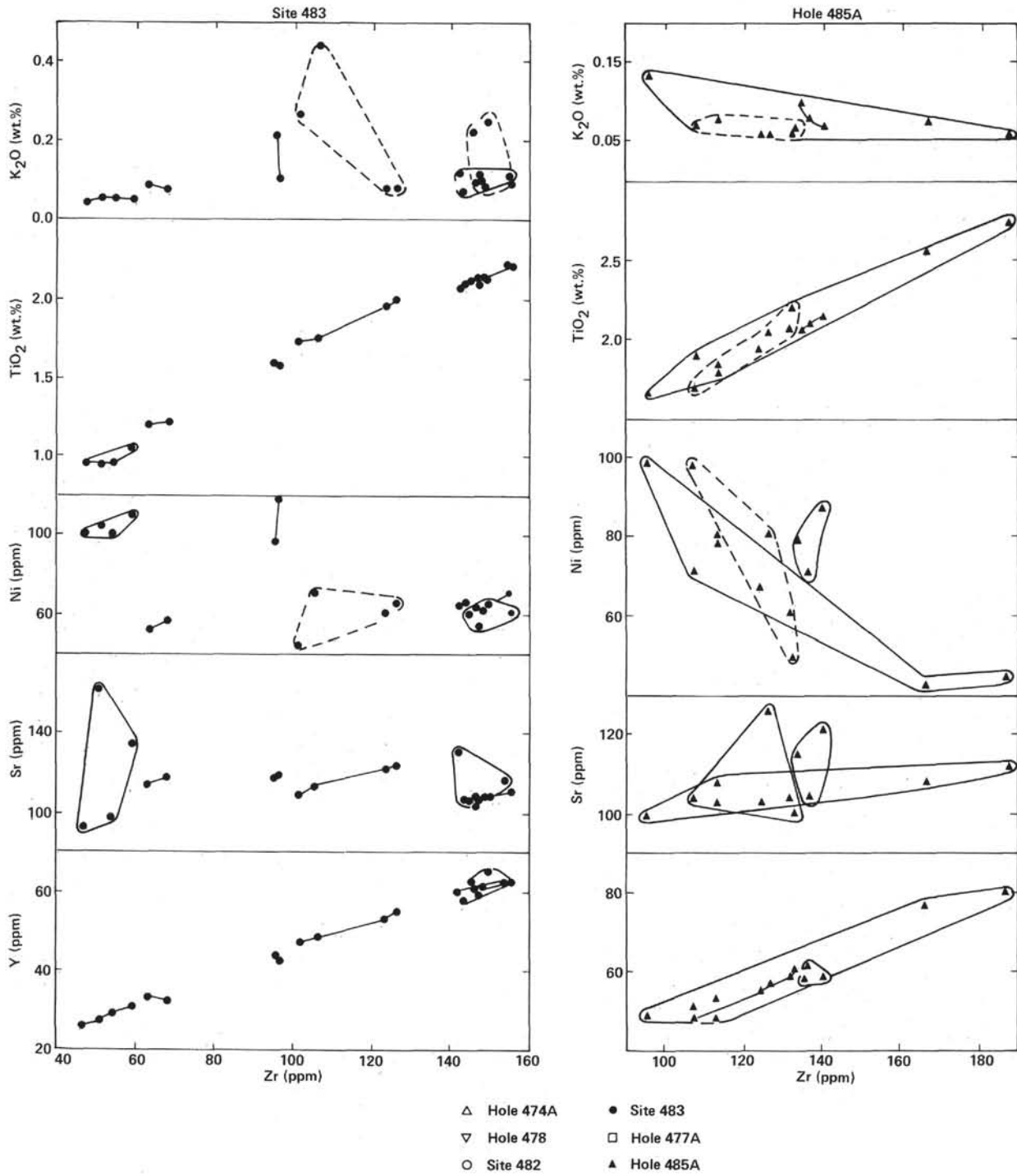


Figure 4. (Continued).

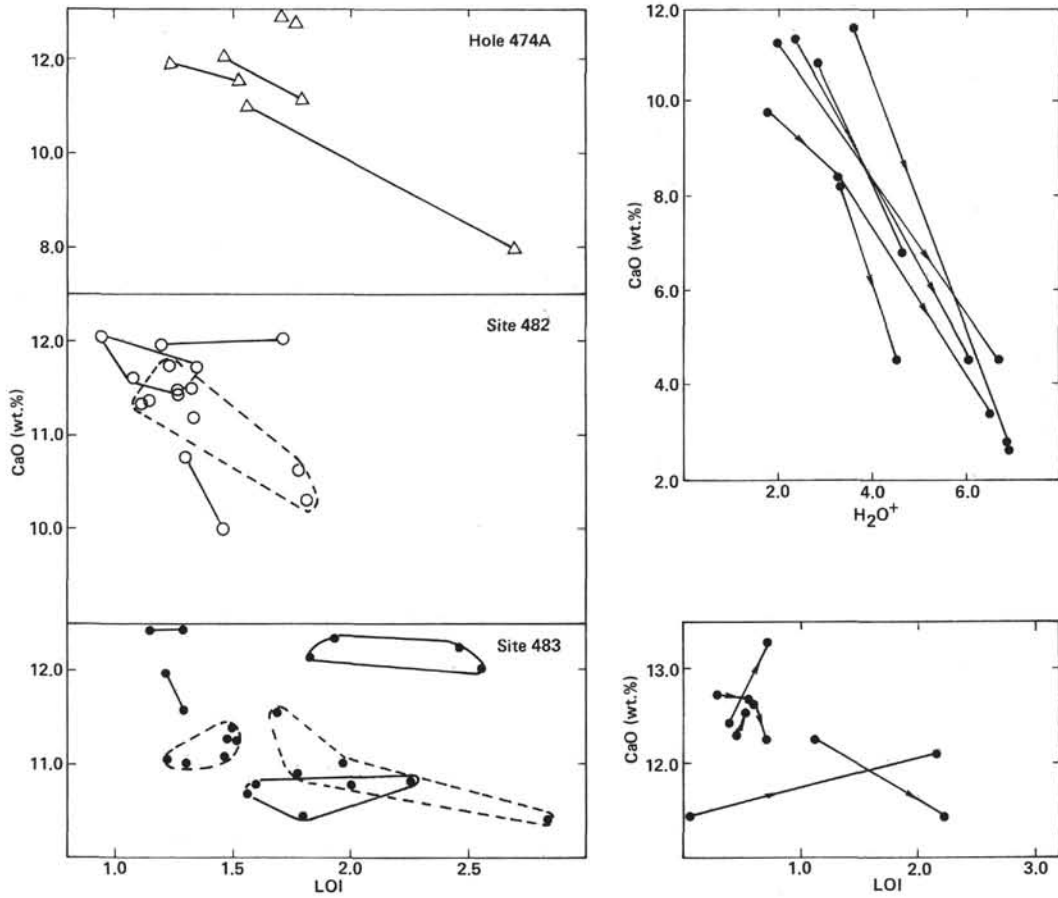


Figure 5. Variation of CaO with loss on ignition (LOI) in selected basalt units from Legs 64 and 65. (For explanation of right-hand diagrams see text.)

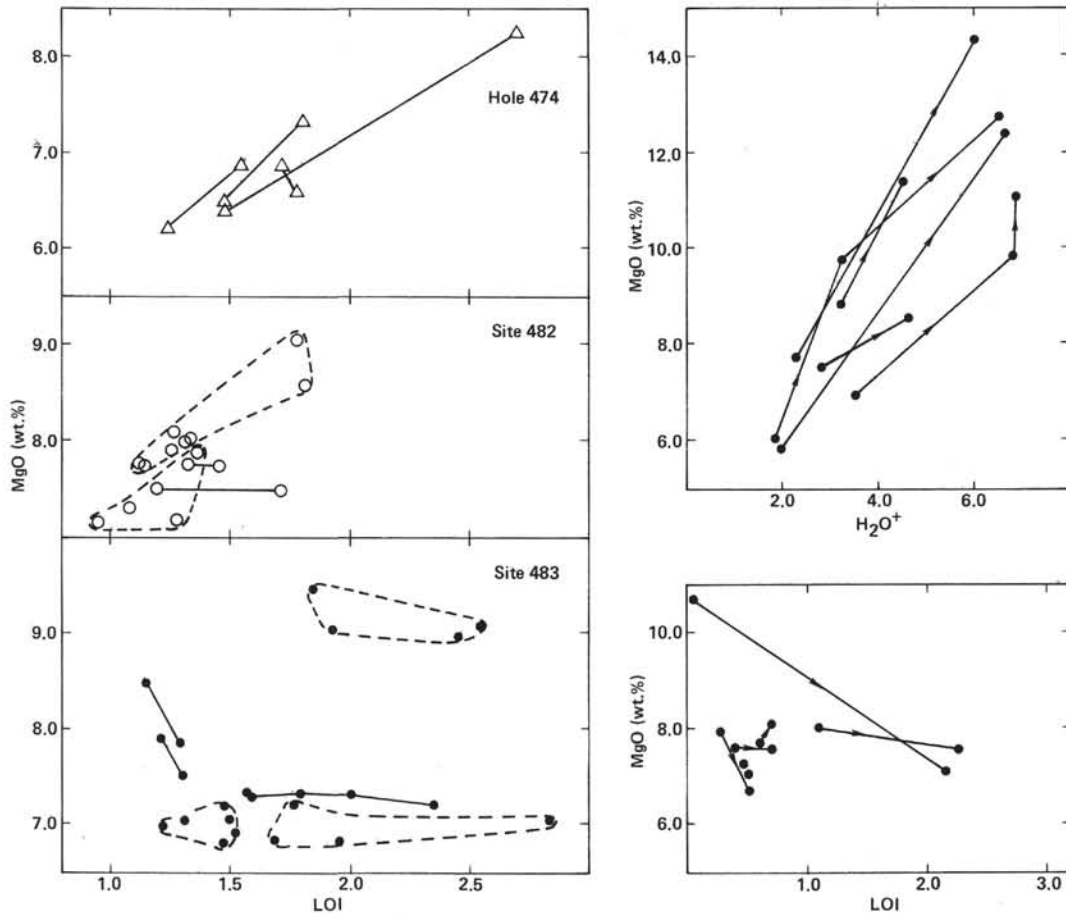


Figure 6. Variation of MgO with loss on ignition (LOI) in selected basalt units from Legs 64 and 65. (For explanation of right-hand diagrams see text.)

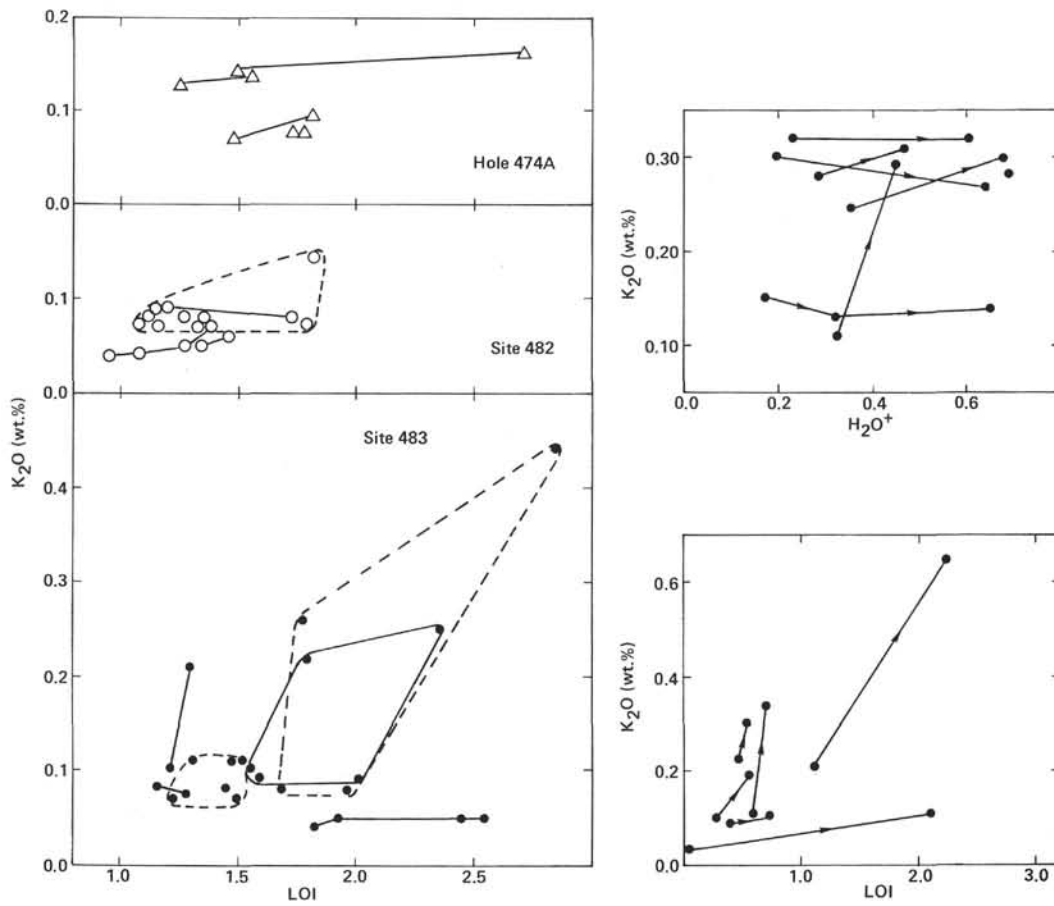


Figure 7. Variation of K<sub>2</sub>O with loss on ignition (LOI) in selected basalt units from Legs 64 and 65. (For explanation of right-hand diagrams see text.)